Toward UO_2 micro/macro machining: a laser processing approach

Thomas Doualle[1], Matthieu Reymond[1,2], Yves Pontillon[1] and Laurent Gallais[2]
[1]CEA, DES, IRESNE, DEC, Cadarache F-13108 Saint-Paul-Lez-Durance, France
[2] Aix Marseille Univ, CNRS, Centrale Marseille, Institut Fresnel, Marseille, France
thomas.doualle@cea.fr

***Abstract*—Linked to experimental data acquisition and to development of improved models, a better detailed description of the behaviour of the nuclear ceramics as regard to the fission gases release during thermal transient representative of nuclear accidents such as RIA (Reactivity Initiated Accident) and or LOCA (LOss of Coolant Accident) requires access to local information within the fuel pellet, and no longer averaged over the whole of the pellet. One of the major challenge in this context is the sample size, which depends on the main objective of the study, typically from the order of a few hundred microns to millimeters. Few techniques allow this dynamic while being compatible with irradiated fuel constraints. Laser micromachining is a high precision non-contact material removal process that would be adapted to this dynamic. We present experimental and numerical studies, carried out in order to evaluate the possibility to apply this process for the preparation of irradiated UO_2 samples of various dimensions. First, preliminary experimental and numerical works conduced on graphite, as model material, which have comparable properties (in particular their behaviours under laser irradiation and their melting point) in order to validate the feasibility, will be detailed. Afterwards, based on these results, we present our first results on UO_2. The objective is to transfer the technique to non-irradiated UO_2 and then to the irradiated material.**

***Keywords* —UO_2, graphite, laser ablation, laser cutting finite element model**

I. Introduction

Lasers are essential tools for macro and micro-processing for a whole range of materials. Processes involving lasers provide a unique solution with minimum mechanical and thermal influence on the processed part due to their selective energy control and deposition and allow generally high processing speeds.

For instance, Pulsed Laser Ablation (PLA) is a technique of vast scientific and significant industrial interest because of its potential applications in micromachining (drilling and cutting), deposition of coatings and thin films, synthesis of a wide range of nanostructures and nanoparticles or surface patterning. With PLA approach, the quality of the processing result is reduced by thermal damage of the workpiece and therefore the quality is increased with shorter pulse duration: the Heat Affected Zone (HAZ) is reduced, leading to higher accuracy. However, ablation efficiency decreases as well. Thus, if high precision is needed, short and ultrashort (femto-, pico- and nanosecond laser) in combination with adequate drilling strategies are applied (such as trepanning). However, single pulse drilling using milli- and microsecond pulses are much more efficient and allow the production of many craters within a short time. The drawback however is the extension of the HAZ, leading to potentially low quality and reproducibility of the craters. In this work, we use a microsecond pulsed laser and the objective was to find the best compromise between the efficiency of the process (ablation rate) and the quality (reduced heat affected zone).

Our approach is based on the one hand on experiments involving a monomode kW Ytterbium fiber laser, and on the other hand on a numerical model to improve the understanding of the underlying physical phenomena and processes involved. These results, obtained on graphite, will be used as a first step towards machining nuclear fuels, such as UO_2, allowing sample preparation for various applications (annealing tests, mechanical behaviour or thermophysical properties).

In this paper, we present in Sec. II the experimental details which enable us to heat up graphite material above sublimation temperature and hence locally ablate material from graphite surface. Section III is dedicated to the description of the model developed to understand the typical crater profiles obtained with our microsecond laser ablation/cutting approach. In Sec. IV, we discuss about the results. First, we describe single-pulse laser ablation and the evolution of the crater dimensions as a function of the laser power. To improve the understanding of the experimental results (craters dimensions and morphology), we compare the simulations results to the experimental crater dimensions. Secondly, we describe a laser cutting technique and its performances which could be applied for graphite manufacturing. Finally, we present the first single pulse ablation experiments on UO_2.

II. Experimental setup

A. Samples

The experiments were conducted on the EDM-3 graphite from POCO Graphite Inc., which is a polycrystalline graphite produced by sintering [1]. The UO_2 samples were fabricated at CEA. Samples have a disk morphology with a diameter of 8 mm and their thicknesses vary from 0.5 to 1.5 mm.

B. *Experimental setup*

For the experiments, an Ytterbium fibre laser (redPOWER Qube 1.5 kW, SPI Lasers), which has a central wavelength of 1080 nm with a bandwidth < 4 nm, with a maximum output power of 1500 W is used. A high power laser collimator generates a 13.5 mm diameter Gaussian beam that is injected in a 2D scanning head composed by two galvanometer mirrors (intelliSCAN 20, ScanLab). The experimental configuration is represented in Figure 1 (a). The laser beam is focused using a F-theta lens with a focal length of f = 255 mm and the working distance, i.e. the distance between the exit of the focusing lens and the nominal working plane, is 303 mm. In this plane, the laser beam was measured with a beam profiler (Beamage 4M, Gentec) and the diameter at $1/e^2$ is 40 µm. The typical image field size is 110 x 110 mm^2. The maximum marking speed of our scanning head is 1 m/s with a repeatability < 2 µrad. A commercial laser machining software (LaserDesk, Scanlab) is used to control and generate the movements of the mirrors and ensure the synchronization with the laser irradiation. The laser power was calibrated with a power calorimeter (Gentec, UP55C-2.5KW-HD-D0). For the experiments conducted under vacuum atmosphere (on UO_2 samples), the laser beam is focused in a vacuum chamber (X40K, Neyco), equipped with a UV fused silica window (WG41050-C, Thorlabs) which has an antireflection coating for the laser wavelength. The operating pressure is close to 10 mbar. The experiments on graphite were carry on under air.

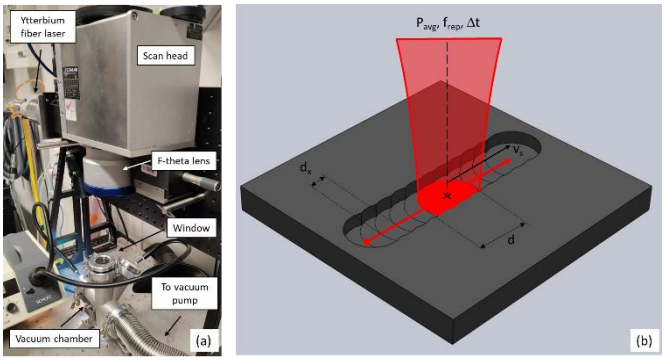

Fig. 1. (a) Experimental configuration (b) Illustration of the process parameters involved during laser processing

The main process parameters for ablating and cutting graphite sample with pulse laser irradiation are shown schematically in Figure 1 (b). The laser beam has a power of P, a pulse duration Δt, a repetition rate f_{rep}, and is focused on a diameter d (gaussian beam, defined at $1/e^2$). It is moved across the graphite surface at the scan speed v_s in a unidirectional scan pattern resulting in a distance d_x between each pulse:

$$d_x = \frac{v_s}{f_{rep}}, \tag{1}$$

The ablation depth z_{ab} is determined as the height difference between the initial surface and the bottom of the ablated area and the ablated width w_{ab} corresponds to the diameter of the individual hole generated by each pulse.

C. *Characterizations*

Regarding sample characterizations, surface observations are carried out employing an optical microscope (Axiotech, Zeiss) and a scanning electron microscope (TM 1000, Hitachi) to investigate the morphology of craters and structures formed and measure their dimensions.

III. Modeling

Simulations are conducted with the commercial software COMSOL, which is based on the Finite Element Method, in axisymmetric configuration, with a two dimensional meshing, to go further in the investigation and understand the laser ablations mechanisms. Heat transfer by conduction associated with deformed geometry and ray-tracing modules are employed for the analysis of the thermal effects, material evaporation and laser propagation on the fabricated structures.

The heat transfer model relies on several assumptions. First, the graphite is considered homogeneous and isotropic. Second we take into account the heat transfers by conduction combined with thermal radiation to take into account losses at the surface (convection is neglected). Third, as the energy is absorbed on the surface, there is no heat source in the material but an incoming heat flux on the boundary, deduced from a ray tracing approach. The corresponding non-linear heat transfer equation can be expressed as:

$$\rho(T)C_p(T)\frac{\partial T}{\partial t} + \nabla(-k(T)\nabla T) = 0, \tag{2}$$

where ρ is the density, C_p is the specific heat capacity under constant pressure, T is the temperature, k is the thermal conductivity. The thermal model and its associated input parameters presented in this paper are based on the model described and validated up to 3800 K in previous study [2].

The laser beam is discretized in rays transporting an amount of energy and computed, one by one, through ray propagation and interactions between the material and the geometry.

To simulate the crater formation, we have taken into account in the numerical model the velocity of the evaporation front at the sample surface, given by [3]:

$$v(T) = \beta\sqrt{\frac{M}{2\pi RT}}\frac{p_{sat}(T)}{\rho(T)}, \tag{3}$$

To investigate the crater formation dynamics, we have used a moving boundary condition at the sample surface, controlled by the local evaporative velocity, associated with a moving mesh functionality in the 2D numerical model.

Evaporative cooling is included as a surface boundary condition since it can be a significant heat transport mechanism as the temperature comes closer to the sublimation point. The outgoing heat flux at the boundary can be obtained as [2]:

$$\varphi(T) = \beta\sqrt{\frac{M}{2\pi RT}}\frac{\Delta H_v}{R}p_0 exp\left[\frac{\Delta H_v}{R}\left(\frac{1}{T_v}-\frac{1}{T}\right)\right], \tag{4}$$

with M being the molar mass of carbon, R the perfect gas constant, ΔH_v the enthalpy of the phase change, T_v the temperature of the phase change at ambient pressure p_0. The input parameters used in this last equation are given in [4].

IV. Results and Discussions

A. *Single pulse ablation on graphite*

Pulse laser ablation results in a crater formation on the solid matter surface. The observation and the description of crater is an interesting method to understand the physics of the ablation on the material of interest. We have coupled this experimental

study with numerical simulations to improve the understanding of the results.

Figure 2 shows craters that are produced on graphite by using single-pulse ablation process with increasing laser power. The pulse duration was 50 µs. This is the shortest pulse possible duration that the laser can produce and we have chosen it to minimize the heat effects.

The top-views show that the entrance craters are extremely clean and present an excellent definition with very little evidence of collateral thermal effects. It is interesting because for most of materials, microsecond pulses involve many collateral effects that can affect the quality of the structure like a large HAZ, a recast layer, micro-cracks, shock waves surface damages and debris from ejected material.

The cross-sections observations highlight the "channel" shape of the hole. The Figure 3 presents the results of the simulations in the case of laser power during 50 µs, which corresponds to the experimental crater represented in the Figure 2 (a) and (f).

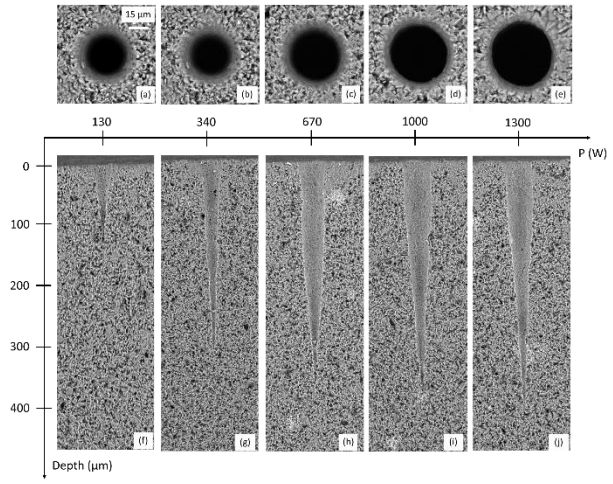

Fig. 2. SEM measurements of craters obtained at different laser powers. (a) to € and (f) to (j) are respectively top and cross-section views. The duration of the laser pulses is 50 µs.

Although, the simulated crater at the end of the irradiation does not have the tapered morphology, we note that dimensions (width and depth) obtained are comparable. Furthermore, as represented on the right part of the Fig. 3, the rays, after one reflection (black rays), which still contain a non-negligible energy (reflection is 8.5 + 0.5%), propagate in the direction of the centre of the hole. This can explain the high-aspect ratio of the crater and its tapered shape observed experimentally.

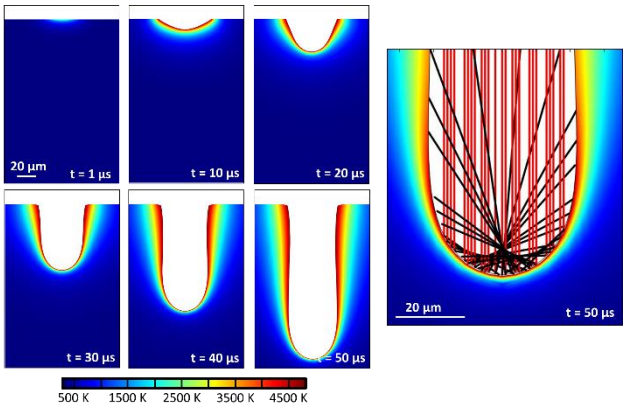

Fig. 3. Simulations of the distribution of temperature, the geometry deformation and the ray propagation in the graphite material at different time (from 1 µs to 50 µs) for a laser power of 130 W.

To go further, we have extended this numerical study by increasing the laser power. The Figure 4 represents the simulated (blue and black dashed lines) and experimental (blue and black dots) results of the ablated depth z_{ab} and width w_{az} of the craters as a function of laser power applied.

We note that the crater width increases with the laser power to reach a value close to the beam diameter. Considering experimental uncertainties, the calculated crater width (represented by the black dashed line) are close and follows the same trend as the experimental ones.

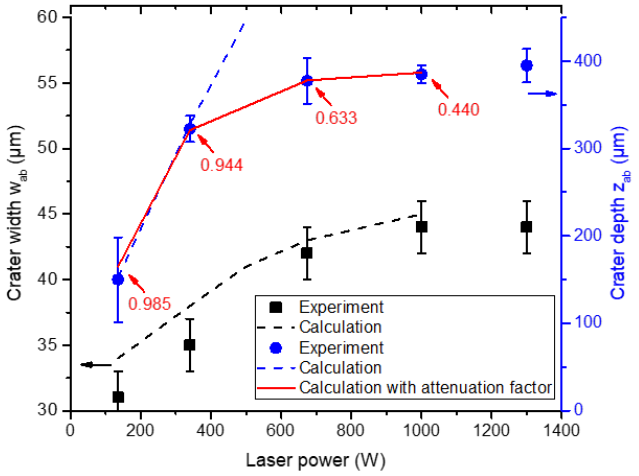

Fig. 4. Experimental crater depth z_{ab} (blue dots) and diameter w_{ab} (black dots) as a function of laser power. The black and blue dashed lines are the corresponding numerical results. The red line indicates the depths obtained with the model considering the attenuation factors (the numerical values are indicated for each power).

Regarding the experimental crater depth evolution, it increases with laser power then shows a trend of saturation. The good agreement with experiments is obtained in the lowest power range, leading to crater depth up to 300 µm. For higher powers, discrepancy is observed. This is probably correlated to a strong material ejection and the formation of a vapour plume which leads a partial screening of the laser power at the sample surface. This phenomenon is not considered in our model and it is certainly a limitation of our approach. However, to take into account the attenuation of the laser resulting from the vapour plume, we could incorporate in the incident laser beam equation an attenuation factor which would depend, for example, on the ablation depth or the laser power. Sinha [5] presented a theoretical model which takes into account a residual attenuation of the laser (resulting of the ejected vapour plume). In our case, we can deduce an attenuation factor, for each laser power. It corresponds to the coefficient which should have been multiplied to the laser power in the entry of the model to obtain the experimental depth. The numerical values of these factors are indicated in Figure 4 and the corrected depths, considering these attenuation factors, are represented by the red line.

B. Cutting on graphite

From the single pulse ablations presented in Sec. IV. A, we propose a laser cutting technique which could be applied for graphite manufacturing. The cutting process technique

developed in our laser facility involves overlapping series of individual craters generated by each pulse.
The spot overlap is crucial in laser cutting because it has a direct impact on the cut quality or on the width of laser cut. We conducted a parametric study which optimized the spot overlap to cut 1.5 mm thick graphite samples. The laser processing parameters are: laser of 1300 W, laser frequency of 0.25 kHz, scan speed of 0.25 mm/s and pulse duration of 50 µs.
We fabricated high aspect ratio shapes in graphite samples of 1.5 mm thickness, as represented in Figure 5.

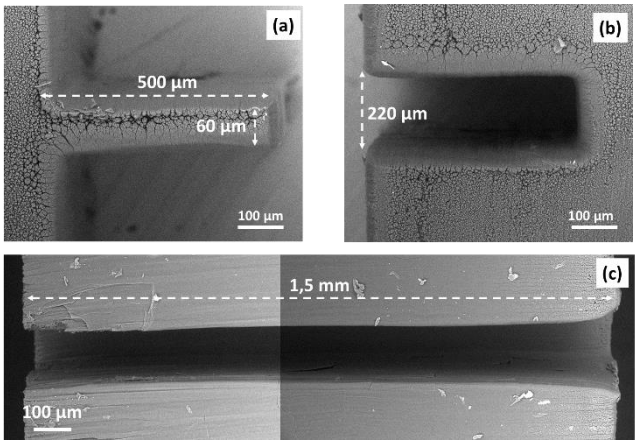

Fig. 5. SEM measurements of a pattern. (a) and (b) are top-views and (c) is the corresponding cross-section view of the part observed in (b).

The desired pattern was a narrow trench with a width of 150 µm and a depth of 500 µm in the 1.5 mm thickness graphite sample. The top-views SEM observation of the two cut parts show the proper contour of the cutting in Figure 5 (a) and (b). We note the difference between the width of the two parts: 220 µm – 60 µm = 160 µm which corresponds to the kerf width during the laser cutting.
The cross-section view, on the Figure 5 (c), shows the homogeneity of the trench width throughout the sample thickness. These parts, and particularly the one on Figure 5 (a) demonstrate the capacity of the laser cutting technique to fabricate high aspect ratio parts (here more than 8) with a good balance between the relative simplicity of technique implementation and its high cutting speed. For this thickness sample graphite of 1.5 mm, the cutting pattern is realized in around 4.5 s.

C. Pulse laser ablation on UO_2

From these results on graphite, we transferred the laser ablation technique to non-irradiated UO_2. Our approach is similar: study the behavior of the material with single-pulsed ablation and then overlap the craters to form a trench. We present here the first step, *i.e.* single pulse laser ablation on UO_2.
The experimental configuration remains identical except that we use a chamber to carry out the ablations under vacuum atmosphere to avoid oxidation and to control the evaporating gases during the processing.
The Figure 6 are top-views SEM observations of single pulse ablation on UO_2 with an increasing laser power. The laser pulse duration was 50 µs, still with the idea to minimize the thermal effects. As observed on the graphite, the higher is the laser power, the larger is the crater until reaching a trend of saturation which corresponds to the diameter of the laser beam.

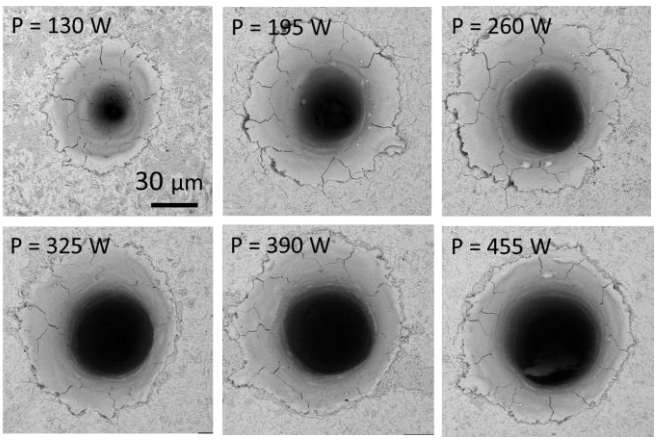

Fig. 6. Top-view SEM measurements of craters obtained at different laser powers.

Although the crater quality is not directly comparable with the craters obtained on the graphite, these results are encouraging because the collateral effects are limited: there is observable no micro-cracks or shock waves surface damages or debris from ejected material. However, we can observe than the HAZ is larger and an observable recast layer around the crater that cannot be neglected.

V. Conclusion and perspectives

As a conclusion, laser micro-processing of graphite employing an Ytterbium fibre laser delivering microsecond pulses at 1080 nm has been experimentally investigated, with the support of a numerical model to investigate and understand the laser ablation mechanisms processes. Firstly, studies were conducted on single-pulse laser ablations with a minimum pulse duration of 50 µs and various power levels up to 1300 W with a beam diameter of 40 µm. The crater depth was found to increase firstly linearly with laser power, in good agreement with the simulation results, then followed by a saturation trend that we attribute to the effect of screening by the vapour plume. Based on these results, we have shown that such laser cutting technique can produce parts with excellent quality (reduced affected area, no recast layer, no micro-cracks and no debris from ejected material) with high efficiency. Production of parts with high aspect ratio were demonstrated, with a cutting depth of 1.5 mm.
From this works on graphite, we consider to transfer this laser ablation technique to nuclear fuels. In this context, we presented first micro-second pulse laser ablation experiments on UO_2. We observe that the crater quality is correct which encourages us to continue the experiments especially using the same approach than of graphite: perform a parametric study of the laser processing parameters to optimize the overlap between two craters and find a UO_2 laser cutting procedure which gives the smallest thermal affected area and the highest precision machining kerf. It can be also envisaged to perform experiments with shorter pulsed lasers (pico and femtosecond) in order to reduce the improve the precision and minimize the HAZ.

REFERENCES

[1] Poco Graphite, Inc. “Properties and Characteristics of Graphite for the EDM Industry”, Edited by R. G. Sheppard, Dwayne Morgan, D. M. Mathes, D. J. Bray, 5th Printing (2002).
[2] L. Gallais, T. Vidal, E. Lescoute, Y. Pontillon and J.L. Rullier, “High power continuous wave laser heating of graphite in a high temperature range up to 3800 K”, Journal of Applied Physics, vol 129, pp. 043102, 2021, doi.org/10.1063/5.0033530
[3] L. Robin, P. Combis, P. Cormont, L. Gallais, D. Hébert, C. Mainfray and J.L. Rullier, “Infrared thermometry and interferential microscopy for analysis of crater formation at the surface of fused silica under CO2 laser irradiation”, Journal of Applied Physics, vol 111, pp. 063106, 2012, doi.org/10.1063/1.3695375
[4] D. Lee, R. Patwa, H. Herfurth, J. Mazumder, “High speed remote laser cutting of electrodes for lithium-ion batteries: Anode”, Journal of Power Sources 240, pp. 368 – 380, 2013, doi.org/10.1016/j.jpowsour.2012.10.096
[5] S. Sinha, “Nanosecond laser ablation of graphite: A thermal model based simulation”, Journal of Laser Applications 30, pp. 012008, 2018, doi.org/10.2351/1.5021520